Proteomic profiling enables prediction of novel senolytics from large-scale drug screens

Alireza Delfarah[1], DongQing Zheng[1], James H. Joly[1], Jesse Yang[1] and Nicholas A. Graham[1,2,3]

[1] Mork Family Department of Chemical Engineering and Materials Science,

[2] Norris Comprehensive Cancer Center,

[3] Leonard Davis School of Gerontology,

University of Southern California, Los Angeles, CA 90089

Running title: *Proteomic profiling enables prediction of novel senolytics*

Corresponding author: Nicholas A. Graham, University of Southern California, 3710 McClintock Ave., RTH 509, Los Angeles, CA 90089. Phone: 213-240-0449; E-mail: nagraham@usc.edu

Abstract

Cellular senescence is the natural program by which cells enter a permanent cell cycle arrest in response to stresses including replicative exhaustion, oncogenic signaling, or DNA damage. Although senescence exerts beneficial effects by acting as a barrier against tumorigenesis, senescent cells can also drive chronic inflammation and age-related diseases through secretion of cytokines and other inflammatory proteins. Therefore, the identification of senolytic compounds that specifically eliminate senescent cells has become an area of great therapeutic promise. Here, we used mass spectrometry-based proteomics to identify senescence biomarkers in primary human mammary epithelial cells (HMECs), a model system for aging. By integrating proteomic data from replicative senescence, immortalization by telomerase reactivation, and drug-induced senescence, we identified a robust HMEC proteomic signature of senescence consisting of 57 upregulated and 29 downregulated proteins. This senescence signature identified both well-known senescence biomarkers, including downregulation of the nuclear lamina protein lamin-B1 (LMNB1), as well as novel biomarkers such as upregulation of the β-galactoside-binding protein galectin-7 (LGALS7). Then, we integrated our proteomic signature of senescence with large-scale drug screening databases to predict that EGFR inhibitors, MEK inhibitors, and dasatinib are novel senolytics in HMEC. Taken together, our results support that the combination of quantitative proteomics and public drug screening databases is a powerful approach to identify senescence biomarkers and novel senolytic compounds.

Introduction

Cellular senescence is a complex stress response that results in permanent cell cycle arrest. Multiple stressors can induce senescence, including replicative stress (e.g., telomere attrition), DNA damage (e.g., DNA double strand breaks), reactive oxygen species, oncogene activation, and even drug-induced stress (Campisi 2013). Senescence plays a role in development (Muñoz-Espín et al. 2013; Storer et al. 2013) and wound healing (Demaria et al. 2014; Jun & Lau 2010) but is most famous as a protective stress response against cancer (Collado & Serrano 2010). However, as senescent cells accumulate in aging tissues (Krishnamurthy et al. 2004), they drive multiple age-related pathologies including atherosclerosis (Childs et al. 2016), cardiac dysfunction (Demaria et al. 2017), diabetes (Thompson et al. 2019), kidney dysfunction (Valentijn et al. 2018), osteoarthritis (Jeon et al. 2018), and overall decrements in healthy lifespan (Baker et al. 2016; Baker et al. 2011). Many of the pro-disease effects of senescence are mediated by the senescence-associated secretory phenotype (SASP), a complex mixture of cytokines secreted by senescent cells that promote inflammation, wound healing, and growth responses in nearby cells (Tchkonia et al. 2013; Tominaga 2015).

Senolytic drugs are agents that selectively induce death of senescent cells. Given their role in age-related disease, the targeted elimination of senescent cells using senolytic drugs is an active area of basic and translational research (Kirkland et al. 2017; Childs et al. 2015; Kirkland & Tchkonia 2020). Since the identification of dasatinib and quercetin as the first senolytic drugs (Zhu et al. 2015), rapid progress has been made in identification of other senolytic drugs including HSP90 inhibitors (Fuhrmann-Stroissnigg et al. 2017), the BCL-2 / BCL-xL inhibitor navitoclax (Zhu et al. 2016; Chang et al. 2016), the naturally-occurring flavonoid polyphenol fisetin (Yousefzadeh et al. 2018), FOXO4-p53 interfering peptides (Baar et al. 2017), and others. Cell-based therapies including chimeric antigen receptor (CAR)-expressing T cells that recognize senescent cells have also shown great promise as senolytic agents (Amor et al. 2020). Importantly, however, senolytic compounds vary by cell type. For example, the

combination of dasatinib plus quercetin is senolytic in adipocytes but not in human umbilical vein endothelial cells (HUVECs), whereas navitoclax but not dasatinib plus quercetin is senolytic in HUVECs but not adipocytes (Zhu et al. 2016; Zhu et al. 2015). The cell type-specificity of senolytics is not surprising because the molecular mechanisms underlying senescence and SASP depend on the senescence inducer and cell type (Basisty et al. 2020; Casella et al. 2019). Therefore, continued progress in the characterization of senescent cells and the identification of cell type-specific senolytic compounds is imperative to improve aging and disease through senolytic therapies.

One limitation to the therapeutic targeting of senescent cells has been the lack of robust senescence biomarkers. The identification of cell type-specific senescence biomarkers is particularly essential for therapeutic approaches such as CAR-T cells or drug-loaded nanoparticles that kill senescent cells on the basis of molecular recognition (Amor et al. 2020; Muñoz-Espín et al. 2018). Liquid chromatography-mass spectrometry (LC-MS) proteomics offers the potential for unbiased, quantitative profiling of biological systems at the protein level (Aebersold & Mann 2016). Proteomic approaches are particularly important for the characterization of senescence because of the frequent discordance between RNA and protein expression (Zhang et al. 2014). In this study, we used LC-MS-based proteomics to characterize the proteome of senescent primary human mammary epithelial cells (HMECs). These normal diploid cells have been previously shown to accurately represent the molecular changes that occur during replicative senescence *in vivo* (Stampfer et al. 2013). By integrating proteomic data across three data sets, we identify a core HMEC senescence signature of 86 proteins. This signature includes both well-characterized senescence biomarkers (e.g., downregulation of lamin B1) and novel biomarkers of senescence (e.g., upregulation of LGALS7 (galectin-7)). By integrating our proteomics signature of senescence with large-scale drug screening efforts in cancer cell lines (Corsello et al. 2020; Ghandi et al. 2019), we predict that EGFR inhibitors (e.g., dacomitinb, AZD8931), MEK inhibitors, and the tyrosine kinase inhibitor dasatinib are novel senolytic drugs in senescent HMECs. Taken together,

our results identify novel biomarkers of senescence in primary HMECs and demonstrate that -omics

profiling can be used to infer senolytic compounds from public drug screening databases.

Results

Replicative senescence alters the HMEC proteome

To identify protein biomarkers of replicative senescence, we analyzed primary human mammary epithelial cells (HMECs) using quantitative, label-free LC-MS-based proteomics. We have previously found that HMECs enter senescence at ~40 population doublings (PD) (Fig. 1A) and exhibit molecular markers of senescence including upregulation of senescence-associated β-galactosidase (SA-β-gal), upregulation of the cell cycle inhibitor p21, and cessation of DNA synthesis (Delfarah et al. 2019). Comparing proliferating and senescent HMECs with LC-MS, we measured 1,234 proteins in two independent biological replicates (Fig. 1B and Table S1). Of these proteins, 55 were significantly upregulated and 34 were significantly downregulated in senescent HMECs (FDR-corrected p-value < 0.01 and average absolute $\log_2$ fold change > 1) (Fig. 1C). Among the most upregulated proteins in senescent cells was annexin A1 (ANXA1), which is associated with aging in the rat prostate (Das et al. 2013). Additionally, the β-galactosidase GLB1, which is associated with SA-β-gal activity (Lee et al. 2006), was significantly upregulated in senescent HMECs. Significantly downregulated proteins in senescent HMECs included histone H4 (HIST1H4A) and SLC3A2 (also known as 4F2), a component of several heterodimeric amino acid transporter complexes including the cystine-glutamate antiporter xCT. Hierarchical clustering of the individual sample values for significantly changing proteins demonstrated high reproducibility across biological and technical replicates (Fig. 1D). Next, to understand the functional classes of proteins altered upon replicative senescence, we performed gene ontology (GO) enrichment analysis. The most significantly upregulated GO terms in senescent HMECs included vesicle, extracellular organelle, lysosome, and vacuole, consistent with the known upregulation of secretory pathways and lysosomes in senescence (Fig. 1E, Table S2) (Coppé et al. 2010). The most significantly downregulated GO terms in senescent cells were ribosomal, translational, and RNA-related terms, consistent with reports that reduced RNA turnover and alterations in translation drive cellular senescence

(Mullani et al. 2020; Gonskikh & Polacek 2017). Taken together, our proteomic profiling reveals significant changes in the proteome of senescent HMECs including upregulation of secretory pathways and downregulation of protein translation.

The proteome of hTERT-immortalized HMECs resembles that of proliferating HMECs

We have previously shown that expression of human telomerase reverse transcriptase (hTERT) immortalizes HMECs and enables bypass of replicative senescence (Delfarah et al. 2019). We thus used LC-MS proteomics to compare hTERT-immortalized HMECs to senescent HMECs expressing the negative control protein luciferase. At ~60 days in culture, corresponding to 35 and 85 PD for luciferase and hTERT, respectively, hTERT-expressing HMECs continue to proliferate but luciferase-expressing HMECs are senescent (Fig. 2A). By performing LC-MS proteomic analysis on hTERT-expressing and luciferase-expressing HMECs in technical duplicate, we quantified 1,436 proteins (Table S3), of which 142 and 126 were significantly upregulated and downregulated, respectively, in senescent luciferase-expressing HMECs (Fig. 2B). Interestingly, we found that five members of the lipid regulatory protein family of annexins were significantly upregulated in senescent luciferase-expressing HMECs: ANXA1, ANXA2, ANXA3, ANXA4, and ANXA5. Among the most downregulated proteins were the nucleolar RNA helicase DDX21 and the nuclear lamina component lamin-B1 (LMNB1), both of which have decreased expression in other senescence models (Freund et al. 2012; Lessard et al. 2018). Consistent with results from replicative senescence (Fig. 1), GO enrichment analysis revealed that vesicle, extracellular organelle, lysosome, and vacuole were significantly enriched in senescent luciferase-expressing HMECs, whereas mRNA metabolic processes, ribonucleoprotein complex, RNA binding, and RNA splicing were among the most significantly downregulated GO terms in senescent luciferase-expressing HMECs (Fig. 2C, Table S4). Lastly, we compared the proteomic signature of proliferating hTERT-expressing versus senescent luciferase-expressing HMECs to replicative senescence and found that the signatures were broadly correlated (Pearson's r = 0.71) (Fig. 2D). Notably, two members of the cathepsin family of proteases, CTSA and CTSD, were significantly upregulated in both data sets. Several proteins were

significantly downregulated in both data sets including SLC3A2, the serine protease HTRA1, lamina-associated polypeptide 2 (TMPO, also known as thymopoietin or LAP2), and histone H1.5 (HIST1H1B). Taken together, proteomic analysis of hTERT-immortalized HMECs compared to senescent luciferase-expressing HMECs revealed broad similarity to replicative senescence both at the individual protein and pathway level.

The proteome of RRM2 inhibition-induced senescence resembles that of replicative senescence

We have previously shown that inhibition of the nucleotide synthesis enzyme RRM2 induces senescence in proliferating HMECs (Delfarah et al. 2019). Thus, we next sought to investigate the proteomic signature of RRM2 inhibition-induced senescence. After 3 days of treatment with either DMSO (control) or the RRM2 inhibitor triapine, HMECs were analyzed in biological triplicate using LC-MS proteomics (Fig. 3A). Here, we identified 1,840 proteins (Table S5), of which 32 and 15 were significantly upregulated and downregulated, respectively, in triapine-treated senescent HMECs (Fig. 3B). Galectin-7 (LGALS7), a β-galactosidase-binding protein that can regulate cell-cell and cell-matrix interactions, was the most significantly upregulated protein in triapine-treated senescent HMECs. The tumor suppressor protein p63 (TP63) and the nuclear lamina component lamin-B1 (LMNB1) were among the significantly downregulated proteins in triapine-treated senescent HMECs. GO enrichment analysis revealed that extracellular organelle, vesicle, cytosol, and cytoskeleton were enriched in triapine-treated senescent HMECs (Fig. 3C, Table S6). Conversely, RNA processing, RNA splicing, and nucleoplasm were downregulated GO terms in triapine-treated HMECs. We next compared the proteomic signatures of replicative senescence (Fig. 1) with that of triapine-induced senescence and found that the two signatures were broadly correlated (Pearson's r = 0.65) (Fig. 3D). Several proteins were significantly upregulated in both signatures including ANXA1, LGALS7, and heat shock protein beta-1 (HSPB1). One protein, MCM3, a member of the minichromosome maintenance protein complex (MCM) that is essential for genomic DNA replication, was significantly downregulated in both replicative senescence and triapine-induced

senescence. Taken together, senescence induced by the inhibition of nucleotide synthesis comprises proteomic changes that broadly resemble replicative senescence.

Data integration identifies a proteomic signature of HMEC senescence

To identify a core signature of HMEC senescence, we integrated the proteomic data from replicative senescence (Fig. 1), hTERT immortalization (Fig. 2), and RRM2 inhibition-induced senescence (Fig. 3). In total, 958 proteins were quantified in all three data sets (Fig. 4A and Table S7). Overall, 57 and 29 proteins were significantly upregulated and downregulated across all three senescence signatures, respectively (FDR-corrected p-value < 0.01 and average absolute $\log_2$ fold change > 1). Among the most significantly upregulated proteins were annexin 1 (ANXA1), the tumor suppressor serpin B5 (SERPINB5, also known as maspin), and four members of the cathepsin family of proteases: CTSA, CTSB, CTSD, and CTSZ (Fig. 4B). Among the most downregulated proteins were SLC3A2 (4F2), lamina-associated polypeptide 2 (TMPO), and six individual histones: H1.3 (HIST1H1D), H1.5 (HIST1H1B), H2A.Z (H2AFZ), H2B type 1-J (HIST1H2BJ), H2B type 2-F (HIST2H2BF), and H4 (HIST1H4A). Hierarchical clustering of the individual biological and technical replicates demonstrated consistent upregulation or downregulation for the most significantly changing proteins across the three individual proteomic signatures (Fig. 4C). Next, to identify transcription factors that might regulate senescence, we performed enrichment analysis on the combined proteomics data using transcription factor target (TFT) gene lists (Yevshin et al. 2019) (Table S8). This analysis identified 3 TFTs that were significantly upregulated in senescent HMECs (TFEB, MAFG, PCGF1), and 40 TFTs that were significantly downregulated in senescent HMECs including SUPT20H, SETD1A, and ZFKX3 (Fig. 4D, p-value < 0.05 and FDR q-value < 0.1). Taken together, our combined analysis identified a core proteomic signature of HMEC senescence including potential novel senescence biomarkers and transcription factor regulators of senescence.

Defining a senescence score that predicts HMECs senescence

Having identified an HMEC proteomic signature of senescence, we next asked whether our signature could predict senescence in an independent data set. Because we are unaware of other HMEC proteomic data sets, we turned to transcriptomic profiling data from pre-stasis HMECs (i.e., proliferating), intermediate HMECs, or HMECs at stasis (i.e., a stress-associated senescence barrier associated with elevated levels of p16 and/or p21, G1 arrest, and the absence of genomic instability) (Garbe et al. 2009). We then defined a weighted voting scheme (Golub et al. 1999) where the $\log_2$ fold change of the 86 core senescence proteins (Fig. 4) was multiplied by gene expression data from the same 86 genes. The result is a "senescence score" for each individual sample where increasing scores predict senescence (Fig. 5A). Testing this approach, we found that the senescence score was significantly increased for five independent HMEC cell lines as they entered stasis (Fig. 5B). The average increase in senescence score from pre-stasis to stasis was 3.6 ± 1.4 (p = 0.0014). These results indicate that the senescence score can predict whether HMEC cultures are proliferating or senescent.

Large-scale drug screening databases predict that EGFR inhibitors, MEK inhibitors, and dasatinib are senolytic compounds in HMECs

We next sought to leverage our HMEC proteomic signature of senescence to identify novel senolytic compounds in HMEC. We hypothesized that large panels of molecularly characterized human cancer cell lines (e.g., the Cancer Cell Line Encyclopedia (CCLE)) (Ghandi et al. 2019) paired with large-scale drug screening databases (e.g., PRISM Repurposing Screen from the Cancer Dependency Map (DepMap)) (Corsello et al. 2020) would enable us to identify drugs that are selectively toxic to senescent cells (i.e., senolytic compounds). To test this hypothesis, we first asked whether we could use gene expression data from senescent adipocytes to recapitulate the discovery of dasatinib as a senolytic compound in adipocytes (Zhu et al. 2015). Using the 104 most differentially expressed genes between proliferating and senescent adipocytes ($\log_2$ fold change > 2.5), we first calculated an "adipocyte senescence score" for ~500 cell lines present in both CCLE and the DepMap drug screening databases.

This weighted voting approach is analogous to calculation of the HMEC senescence score (Fig. 5A) except that log_2 fold change values were derived from transcriptomic analysis of proliferating and senescent adipocytes instead of HMEC proteomic profiling. We then correlated the adipocyte senescence score with sensitivity to 1,448 drugs in the DepMap drug sensitivity database (Table S9). Here, because a smaller dose-response area under the curve (AUC) indicates higher sensitivity to the small molecule, compounds with negative correlations are more toxic to senescent cells. Confirming the validity of this approach, the drug whose sensitivity was most negatively correlated with the adipocyte senescence score was dasatinib (FDR-corrected p-value $9x10^{-4}$) (Fig. S1A,B). In contrast, the drug navitoclax, which is senolytic in human umbilical vein epithelial cells (HUVECs) but not in adipocytes, was not significantly correlated with the adipocyte senescence score (FDR-corrected p-value 0.6) (Fig. S1C). Taken together, this confirms that combining senescence signatures with large-scale databases of transcriptomic profiling and drug sensitivity data can be used to identify senolytic compounds.

Next, we applied this approach to discovery of senolytic compounds in HMECs. We first asked whether the 86 proteins in our HMEC proteomic signature of senescence were correlated in the CCLE gene expression data. Strikingly, most of the upregulated HMEC senescence proteins were positively correlated with one another and negatively correlated with the downregulated HMEC senescence proteins (Fig. S2). Analysis of proteomic profiling data from CCLE (Nusinow et al. 2020) revealed similar trends (Fig. S3). These results indicate that the HMEC senescence proteins are co-regulated and could be used to predict an HMEC senescence-like signature in cancer cell lines. Therefore, we calculated the HMEC senescence score for ~500 cancer cell lines present in both the CCLE and the DepMap drug screening databases. Although no voting proteins overlap between HMEC and adipocyte senescence scores, the two senescence scores were significantly correlated (Pearson's r = 0.34) (Fig. S4A). Next, we correlated the HMEC senescence scores with drug sensitivity (AUC) (Fig. 6A, Table S10). Interestingly, the two drugs whose sensitivity was most negatively correlated with the HMEC senescence score (i.e., senolytics) were the EGFR inhibitors dacomitinib and AZD8931 (Fig. 6B,C). Dasatinib but not

navitoclax was also significantly negatively correlated with the HMEC senescence score (Fig. 6B). Conversely, the two drugs whose sensitivity was most positively correlated with the HMEC senescence score were anguidine and indisulum, inhibitors of protein synthesis and cyclin-dependent kinases, respectively (Fig. S4B). This result suggests that these drugs are more toxic to proliferating rather than senescent HMEC. Lastly, we used Drug Set Enrichment Analysis (DrugSEA), a variant of gene set enrichment analysis (GSEA) (Subramanian et al. 2005) that identifies enriched drug targets, to analyze the list of correlation coefficients between HMEC senescence score and drug sensitivity. Overall, both EGFR and MEK inhibitors were significantly negatively enriched, indicating selective toxicity against cell lines with HMEC senescence-like signatures (Fig. 6D, Table S11). Taken together, these results suggest that EGFR inhibitors, MEK inhibitors, and dasatinib are senolytic in HMECs.

Discussion

Cellular senescence is a state of irreversible cell cycle arrest that contributes to degenerative and hyperplastic phenotypes in aging, cancer, and many other diseases. The targeted elimination of senescent cells with senolytic compounds has emerged as a promising therapeutic approach for both disease and healthy aging. Here, we were motivated by the paucity of senescence biomarkers and the need to identify cell type-specific senolytic compounds. First, we used LC-MS proteomics to characterize the proteome of senescent primary HMECs and identified a robust signature of 86 HMEC senescence biomarkers (Fig. 4). Then, we integrated our proteomic signature of HMEC senescence with large-scale drug screening databases to predict that EGFR inhibitors, MEK inhibitors, and dasatinib are novel senolytic drugs for HMEC. Taken together, our study adds to the growing literature on senescence biomarkers, senolytic agents, and computational approaches to identify novel therapeutics from large-scale public databases.

Proteomics has emerged as a powerful tool for the identification of novel senescence biomarkers (Althubiti et al. 2014), proteomic alterations in the aging lung (Angelidis et al. 2019), the therapy-induced senescence proteome (Flor et al. 2017), SASP (Basisty et al. 2020), and signatures of aging in biofluids like plasma (Tanaka et al. 2018; Lehallier et al. 2019). Here, in our HMEC model system of aging, several proteins identified as members of the HMEC senescence proteomic signature are previously known senescence biomarkers. For example, in HMECs, expression of lamin-B1 (LMNB1), a component of the nuclear lamina, was significantly decreased (average $\log_2$ fold change in senescent cells -1.09, FDR-corrected p-value 2.26×10^{-8}). Loss of lamin-B1 expression in senescent cells has been extensively documented, including in replicative senescence, oncogene-induced senescence, and UV-induced senescence (Freund et al. 2012; Dreesen et al. 2013; Sadaie et al. 2013; Shah et al. 2013; Wang et al. 2017). Notably, the lamin-B1-binding partner TMPO (LAP2) was also part of our senescence signature, although decreases in TMPO expression are not unique to senescent cells, as downregulation also

occurs in quiescent cells (Dreesen et al. 2013). Regardless, the concordance of LMNB1 expression in our HMEC system and other studies adds additional support that loss of LMNB1 expression is a bona fide senescence biomarker.

The most upregulated protein in our HMEC senescence signature was the calcium-dependent phospholipid-binding protein annexin 1 (ANXA1) with an average $\log_2$ fold change in senescent cells of 2.35 (Fig. 4B). We also observed significant upregulation of two other annexins, ANXA3 and ANXA5, in senescent HMEC, although these proteins were less upregulated than ANXA1 (average $\log_2$ fold change 1.08 for both proteins). Interestingly, the upregulation of annexins has been previously linked to increased lipid metabolism in a model of therapy-induced senescence (Flor et al. 2017). Moreover, ANXA1 is upregulated in aged rat prostate (Das et al. 2013), accumulation of nuclear ANXA5 is a biomarker of replicative and therapy-induced fibroblast senescence (Klement et al. 2012), and secretion of ANXA1, ANXA3, and ANXA5 is upregulated in senescent fibroblasts (Basisty et al. 2020). In addition, we observed upregulation of several lysosomal proteins in senescent HMEC including GLB1 (β-galactosidase), four cathepsins (CTSA, CTSD, CTSD, and CTSZ), and the glycosylase MAN2B1. These results are consistent with previous reports of increased lysosomal activity in senescence (Nixon et al. 2000; Stoka et al. 2016). Additionally, cathepsins are known to regulate senescence (Byun et al. 2009) and pathogenesis of age-related disease (Nixon et al. 2000) and are also secreted by senescent cells (Basisty et al. 2020). Moreover, the upregulation of ANXA1 and CTSD has been reported as candidate biomarkers of spinal cord injury (Moghieb et al. 2016) which involves the appearance of senescent cells (Pavlicek et al. 2017; Swenson et al. 2019; Takano et al. 2017). Finally, both the β-galactoside-binding proteins galectin-3 (LGALS3) and galectin-7 (LGALS7) were significantly upregulated in senescent HMECs. Galectin-3 can coordinate repair, removal, and replacement of lysosomes (Jia et al. 2020), and its upregulation may reflect attempts by senescent cells to repair deteriorating lysosomes (Park et al. 2018). To our knowledge, galectin-7 has not been reported to be involved in senescence, but we speculate that it may also play a role in lysosomal repair and homeostasis in senescent HMEC. Taken together, these

results suggest that annexins, cathepsins, and galectins are potential senescence biomarkers across many cell types.

The most downregulated protein in our proteomic signature of HMEC senescence was the histone H1.5 (HIST1H1B) with an average $\log_2$ fold change in senescent cells of -2.13 (Fig. 4B). We additionally observed downregulation of five additional histone proteins in our combined proteomics analysis (Fig. 4) including H1.3 (HIST1H1D), H2A.Z (H2AFZ), H2B type 1-J (HIST1H2BJ), H2B type 2-F (HIST2H2BF), and H4 (HIST1H4A). Consistent with our findings, several studies have reported loss of histone H1 and DNA methylation in senescence and aging (Funayama et al. 2006; Heyn et al. 2012; Kane & Sinclair 2019). In addition, increased lysosomal activity has been linked to proteolysis of histones in senescent cells (Ivanov et al. 2013). These results support the regulatory role of chromatin remodeling and reduced DNA methylation in senescence of HMECs.

Our analysis of transcription factors targets (Fig. 4D) revealed significant upregulation or downregulation of several transcription factors that have been previously linked to senescence and aging including downregulation of SETD1A (Tajima et al. 2019), KAT5 (Kwan et al. 2020), and DOT1L (Kim et al. 2012, p.1) as well as upregulation of TFEB (Niu et al. 2019). Interestingly, we also identified significant upregulation of MAFG and PCG1 targets and significant downregulation of NKX2-2, ZFHX3 and SUPT20H targets. To our knowledge, these transcription factors do not have reported roles in aging or senescence. Future studies are necessary to investigate whether these transcription factors are regulators of cellular senescence in HMECs and other cell types.

Senolytics have emerged as an exciting area with great therapeutic promise in aging (Xu et al. 2018; Zhu et al. 2015), cancer (Dörr et al. 2013; Guerrero et al. 2019), and other diseases. In mice, clearance of senescent cells restores tissue homeostasis and delays age-related dysfunction (Baar et al. 2017; Baker et al. 2011; Cai et al. 2020; Baker et al. 2016). Furthermore, clinical trials of the senolytic

combination dasatinib and quercetin have shown encouraging results (Hickson et al. 2019). Our study is the first, to our knowledge, to leverage proteomic or transcriptomic signatures of senescence with large-scale drug screening (e.g., the PRISM drug repurposing resource from DepMap) to predict novel senolytic agents. Although these drug screening is conducted using non-senescent cancer cell lines, the fact that the top hit in our computational analysis of senescent adipocytes was the senolytic drug dasatinib proved the validity of our approach (Zhu et al. 2015) (Fig. S1). Here, based on our proteomic signature of senescence, we predicted that EGFR inhibitors (e.g., dacomitinib, AZD8931), MEK inhibitors, and dasatinib are senolytic agents for HMECs. Interestingly, MEK inhibitors have been shown to eliminate senescent Ras-expressing cells (Kochetkova et al. 2017). Moreover, in IMR90 and HUVECs, the cytokine-mediated induction of senescence can be blocked by pharmacological inhibition or genetic knockdown of EGFR (Shang et al. 2020). Taken together, our results suggest that large-scale drug screening databases are a powerful resource for senolytic discovery in HMECs and other senescence models.

In conclusion, our results support that the combination of quantitative proteomics and public drug screening databases is a powerful approach to identify senescence biomarkers and novel senolytic compounds. Future research into the mechanisms affecting the efficacy and cell-type specificity of senolytic drugs will have important implications for the usage of senolytics in clinical trials. Furthermore, unlocking the transformative power of senolytics will require minimizing off-target effects and an improved understanding of the impact of eliminating senescent cells on health and age-related disease.

Materials and methods

Cell culture

HMEC cells were purchased from Thermo Scientific and cultured in M87A medium (50% MM4 medium and 50% MCDB170 supplemented with 5 ng/ml EGF, 300 ng/ml hydrocortisone, 7.5 µg/ml insulin, 35 µg/ml BPE, 2.5 µg/ml transferrin, 5 µM isoproterenol, 50 µM ethanolamine, 50 µM o-phosphoethanolamine, 0.25 % FBS, 5 nM triiodothyronine, 0.5 nM estradiol, 0.5 ng/ml cholera toxin, 0.1 nM oxytocin, 1% anti-anti, no AlbuMax) in atmospheric oxygen. Glucose and glutamine-free DMEM was purchased from Corning (90-113-PB), Ham's F12 was purchased from US Biological (N8542-12), and MCD170 medium was purchased from Caisson Labs (MBL04). Glucose and glutamine were added to the media at the appropriate concentration for each media type. Cells were lifted with TrypLE at 80-90% confluency and seeded at a density of $2.3 \times 10^3/cm^2$.

LC-MS proteomics

Cell culture dishes were placed on ice and washed with PBS. Cells were then scraped and pelleted by centrifugation. The cell pellets were lysed by probe sonication in 8 M urea (pH 7.5), 50 mM Tris, 1 mM activated sodium vanadate, 2.5 mM sodium pyrophosphate, 1 mM β-glycerophosphate, and 100 mM sodium phosphate. The above procedures were performed in 0-4˚C. Insoluble cell debris were filtered by 0.22 um syringe filter. Protein concentration was measured by BCA assay (Pierce, PI23227). Lysates were reduced with 5 mM DTT, alkylated with 25 mM iodoacetamide, quenched with 10 mM DTT, and acidified to pH 2 with 5% trifluoracetic acid. Proteins were then digested to peptides using a 1:100 trypsin to lysate ratio by weight. Tryptic peptides were desalted by reverse phase C18 StageTips and eluted with 30% acetonitrile. The eluents were vacuumed dried, and 250 ng/injection was submitted to LC-MS. Samples were randomized and injected into an Easy 1200 nanoLC ultra high-performance liquid chromatography coupled with a Q Exactive quadruple orbitrap mass spectrometry (Thermo Fisher). Peptides were separated by a reverse-phase analytical column (PepMap RSLC C18, 2 µm, 100Å, 75 µm

x 25 cm). Flow rate was set to 300 nL/min at a gradient from 3% buffer B (0.1% formic acid, 80% acetonitrile) to 38% B in 110 min, followed by a 10-min washing step to 85% B. The maximum pressure was set to 1,180 bar and column temperature was maintained at 50°C. Peptides separated by the column were ionized at 2.4 kV in the positive ion mode. MS1 survey scans were acquired at the resolution of 70k from 350 to 1800 m/z, with maximum injection time of 100 ms and AGC target of 1e6. MS/MS fragmentation of the 14 most abundant ions were analyzed at a resolution of 17.5k, AGC target 5e4, maximum injection time 65 ms, and normalized collision energy 26. Dynamic exclusion was set to 30 s and ions with charge +1, +7, and >+7 were excluded. MS/MS fragmentation spectra were searched with Proteome Discoverer SEQUEST (version 2.2, Thermo Scientific) against in-silico tryptic digested Uniprot all-reviewed *Homo sapiens* database (release Jun 2017, 42,140 entries) plus all recombinant protein sequences used in this study. The maximum missed cleavages was set to 2. Dynamic modifications were set to oxidation on methionine (M, +15.995 Da) and acetylation on protein N-terminus (+42.011 Da). Carbamidomethylation on cysteine residues (C, +57.021 Da) was set as a fixed modification. The maximum parental mass error was set to 10 ppm, and the MS/MS mass tolerance was set to 0.02 Da. The false discovery threshold was set strictly to 0.01 using the Percolator Node validated by q-value. The relative abundance of parental peptides was calculated by integration of the area under the curve of the MS1 peaks using the Minora LFQ node. The RAW and processed LC-MS files have been uploaded to the PRIDE database (Perez-Riverol et al. 2019) (PXD019057, Username: reviewer29534@ebi.ac.uk, Reviewer password: djc8bohx).

Data processing and normalization

Missing peptide abundances were imputed using the K-nearest neighbor algorithm (Webb-Robertson et al. 2015). The optimized number of neighbors was determined to be n = 10. Protein abundance $\log_2$ ratios and statistical significance were calculated using DEqMS in R software (Zhu et al. 2020). Briefly, peptide sequences were aggregated into protein $\log_2$ ratios by the median sweeping method: raw intensity values were $\log_2$ transformed, the median of $\log_2$ intensity was subtracted for each PSM, and then for each

protein, the relative $\log_2$ ratio was calculated as the median of $\log_2$ ratio of the PSMs assigned to that protein.

Hierarchical clustering

Clustering was performed using Morpheus web tool by the Broad Institute. One minus Pearson correlation coefficient metric was used for clustering. Data was transformed following the clustering by subtracting row mean and dividing by row standard deviation.

Gene Ontology Enrichment Analysis

Proteins were ranked by their $\log_2$ (senescent / proliferating) values, and Gene Ontology 1D-Enrichment analysis was performed in Perseus (version 1.6.2.2).

Transcription Factor Targets Enrichment Analysis

Proteins were ranked by their $\log_2$ (senescent / proliferating) values. Gene Set Enrichment Analysis (GSEA) (Subramanian et al. 2005) was run with the unweighted statistic using the GSEA java applet using Broad Institute C3 TFT:GTRD gene sets.

Senescence score

$\log_2$-transformed, RMA-normalized Entrez gene expression values for adipocyte senescence (GSE66236) were averaged for senescent and proliferating conditions. For each gene, the average value for proliferating samples was subtracted from the average of senescent samples to obtain $\log_2$ (senescent / proliferating) values. Data was filtered for genes with absolute $\log_2$ (senescent / proliferating) > 2.5 to create the adipocyte signature matrix. HMEC senescence signature matrix was created using proteins with absolute average $\log_2$ (senescent / proliferating) > 1 and FDR-corrected p-value < 0.01 of our combined HMEC proteomics analysis (Fig. 4B). CCLE $\log_2$ transformed RNAseq TPM gene expression data for protein coding genes using RSEM "CCLE_expression_v2.csv" was downloaded from DepMap

portal (https://depmap.org/portal/download/). The appropriate genes (i.e., adipocyte or HMEC senescence signatures) were selected to create the CCLE gene expression matrix. CCLE senescence scores vector (of adipocyte or HMEC) was calculated by multiplying senescence signature matrix (of adipocyte or HMEC) with CCLE gene expression matrix.

PRISM analysis

CCLE PRISM Repurposing 19Q4 data "secondary-screen-dose-response-curve-parameters.csv" was downloaded from DepMap portal (https://depmap.org/portal/download/). For each drug, the Pearson correlation coefficient and t-test p-value was calculated between CCLE senescence scores and PRISM area-under-the-curve (AUC) values (only cell lines present in both CCLE gene expression and PRISM Repurposing were used). p-values were corrected for false-discovery rate using the Benjamini-Hochberg method. Drugs with most negative correlation coefficients were selected as potential senolytics. Similar analysis was performed using HMEC or adipocyte senescence signature matrix to calculate CCLE senescence scores and correlate them with PRISM AUC values.

Drug Set Enrichment Analysis (DrugSEA)

DrugSEA is a variant of GSEA designed to identify enriched classes of drug targets. Drugs were mapped to their metabolic pathway using the annotated target(s) and genes from KEGG metabolic pathways. Since the PRISM database contains both activators and inhibitors, we annotated all activators by mechanism of action and multiplied their correlation coefficients by -1. Therefore, a pathway activator would be counted similarly to a pathway inhibitor. Pathways with 4 or more drugs were kept. Then, GSEA was run on the rank lists of 1,448 correlation coefficients.

Acknowledgments

Conflict of Interest Statement

The authors declare no conflicts of interest.

Author Contributions

AD and NAG designed research. AD, DZ, and JY performed research. AD, DZ, JHJ, and NAG analyzed data. AD and NAG wrote the manuscript.

Data Availability Statement

The RAW and processed LC-MS files have been uploaded to the PRIDE database (Perez-Riverol et al. 2019) (PXD019057, Username: reviewer29534@ebi.ac.uk, Reviewer password: djc8bohx).

References

Aebersold R & Mann M (2016) Mass-spectrometric exploration of proteome structure and function. *Nature* 537, 347–355.

Althubiti M, Lezina L, Carrera S, Jukes-Jones R, Giblett SM, Antonov A, Barlev N, Saldanha GS, Pritchard CA, Cain K & Macip S (2014) Characterization of novel markers of senescence and their prognostic potential in cancer. *Cell Death Dis* 5, e1528.

Amor C, Feucht J, Leibold J, Ho Y-J, Zhu C, Alonso-Curbelo D, Mansilla-Soto J, Boyer JA, Li X, Giavridis T, Kulick A, Houlihan S, Peerschke E, Friedman SL, Ponomarev V, Piersigilli A, Sadelain M & Lowe SW (2020) Senolytic CAR T cells reverse senescence‐associated pathologies. *Nature* 583, 127–132.

Angelidis I, Simon LM, Fernandez IE, Strunz M, Mayr CH, Greiffo FR, Tsitsiridis G, Ansari M, Graf E, Strom T-M, Nagendran M, Desai T, Eickelberg O, Mann M, Theis FJ & Schiller HB (2019) An atlas of the aging lung mapped by single cell transcriptomics and deep tissue proteomics. *Nature Communications* 10, 963.

Baar MP, Brandt RMC, Putavet DA, Klein JDD, Derks KWJ, Bourgeois BRM, Stryeck S, Rijksen Y, van Willigenburg H, Feijtel DA, van der Pluijm I, Essers J, van Cappellen WA, van IJcken WF, Houtsmuller AB, Pothof J, de Bruin RWF, Madl T, Hoeijmakers JHJ, Campisi J & de Keizer PLJ (2017) Targeted Apoptosis of Senescent Cells Restores Tissue Homeostasis in Response to Chemotoxicity and Aging. *Cell* 169, 132-147.e16.

Baker DJ, Childs BG, Durik M, Wijers ME, Sieben CJ, Zhong J, A. Saltness R, Jeganathan KB, Verzosa GC, Pezeshki A, Khazaie K, Miller JD & van Deursen JM (2016) Naturally occurring p16 Ink4a -positive cells shorten healthy lifespan. *Nature* 530, 184–189.

Baker DJ, Wijshake T, Tchkonia T, LeBrasseur NK, Childs BG, van de Sluis B, Kirkland JL & van Deursen JM (2011) Clearance of p16Ink4a-positive senescent cells delays ageing-associated disorders. *Nature* 479, 232–236.

Basisty N, Kale A, Jeon OH, Kuehnemann C, Payne T, Rao C, Holtz A, Shah S, Sharma V, Ferrucci L, Campisi J & Schilling B (2020) A proteomic atlas of senescence‐associated secretomes for aging biomarker development. *PLOS Biology* 18, e3000599.

Byun H-O, Han N-K, Lee H-J, Kim K-B, Ko Y-G, Yoon G, Lee Y-S, Hong S-I & Lee J-S (2009) Cathepsin D and eukaryotic translation elongation factor 1 as promising markers of cellular senescence. *Cancer Res.* 69, 4638–4647.

Cai Y, Zhou H, Zhu Y, Sun Q, Ji Y, Xue A, Wang Y, Chen W, Yu X, Wang L, Chen H, Li C, Luo T & Deng H (2020) Elimination of senescent cells by β-galactosidase-targeted prodrug attenuates inflammation and restores physical function in aged mice. *Cell Research* 30, 574–589.

Campisi J (2013) Aging, Cellular Senescence, and Cancer. *Annual Review of Physiology* 75, 685–705.

Casella G, Munk R, Kim KM, Piao Y, De S, Abdelmohsen K & Gorospe M (2019) Transcriptome signature of cellular senescence. *Nucleic Acids Res* 47, 7294–7305.

Chang J, Wang Y, Shao L, Laberge R-M, Demaria M, Campisi J, Janakiraman K, Sharpless NE, Ding S, Feng W, Luo Y, Wang X, Aykin-Burns N, Krager K, Ponnappan U, Hauer-Jensen M, Meng A & Zhou D (2016) Clearance of senescent cells by ABT263 rejuvenates aged hematopoietic stem cells in mice. *Nat. Med.* 22, 78–83.

Childs BG, Baker DJ, Wijshake T, Conover CA, Campisi J & van Deursen JM (2016) Senescent intimal foam cells are deleterious at all stages of atherosclerosis. *Science* 354, 472–477.

Childs BG, Durik M, Baker DJ & van Deursen JM (2015) Cellular senescence in aging and age-related disease: from mechanisms to therapy. *Nat. Med.* 21, 1424–1435.

Collado M & Serrano M (2010) Senescence in tumours: evidence from mice and humans. *Nature Reviews Cancer* 10, 51–57.

Coppé J-P, Desprez P-Y, Krtolica A & Campisi J (2010) The Senescence-Associated Secretory Phenotype: The Dark Side of Tumor Suppression. *Annual Review of Pathology: Mechanisms of Disease* 5, 99–118.

Corsello SM, Nagari RT, Spangler RD, Rossen J, Kocak M, Bryan JG, Humeidi R, Peck D, Wu X, Tang AA, Wang VM, Bender SA, Lemire E, Narayan R, Montgomery P, Ben-David U, Garvie CW, Chen Y, Rees MG, Lyons NJ, McFarland JM, Wong BT, Wang L, Dumont N, O'Hearn PJ, Stefan E, Doench JG, Harrington CN, Greulich H, Meyerson M, Vazquez F, Subramanian A, Roth JA, Bittker JA, Boehm JS, Mader CC, Tsherniak A & Golub TR (2020) Discovering the anticancer potential of non-oncology drugs by systematic viability profiling. *Nat Cancer*, 1–14.

Das A, Bortner JD, Aliaga CA, Baker A, Stanley A, Stanley BA, Kaag M, Richie JP & El-Bayoumy K (2013) Changes in proteomic profiles in different prostate lobes of male rats throughout growth and development and aging stages of the life span. *Prostate* 73, 363–375.

Delfarah A, Parrish S, Junge JA, Yang J, Seo F, Li S, Mac J, Wang P, Fraser SE & Graham NA (2019) Inhibition of nucleotide synthesis promotes replicative senescence of human mammary epithelial cells. *J. Biol. Chem.* 294, 10564–10578.

Demaria M, Ohtani N, Youssef SA, Rodier F, Toussaint W, Mitchell JR, Laberge R-M, Vijg J, Van Steeg H, Dollé MET, Hoeijmakers JHJ, de Bruin A, Hara E & Campisi J (2014) An essential role for senescent cells in optimal wound healing through secretion of PDGF-AA. *Dev. Cell* 31, 722–733.

Demaria M, O'Leary MN, Chang J, Shao L, Liu S, Alimirah F, Koenig K, Le C, Mitin N, Deal AM, Alston S, Academia EC, Kilmarx S, Valdovinos A, Wang B, de Bruin A, Kennedy BK, Melov S, Zhou D, Sharpless NE, Muss H & Campisi J (2017) Cellular Senescence Promotes Adverse Effects of Chemotherapy and Cancer Relapse. *Cancer Discov* 7, 165–176.

Dörr JR, Yu Y, Milanovic M, Beuster G, Zasada C, Däbritz JHM, Lisec J, Lenze D, Gerhardt A, Schleicher K, Kratzat S, Purfürst B, Walenta S, Mueller-Klieser W, Gräler M, Hummel M, Keller U, Buck AK, Dörken B, Willmitzer L, Reimann M, Kempa S, Lee S & Schmitt CA (2013) Synthetic lethal metabolic targeting of cellular senescence in cancer therapy. *Nature* 501, 421–425.

Dreesen O, Chojnowski A, Ong PF, Zhao TY, Common JE, Lunny D, Lane EB, Lee SJ, Vardy LA, Stewart CL & Colman A (2013) Lamin B1 fluctuations have differential effects on cellular proliferation and senescence. *J Cell Biol* 200, 605–617.

Flor AC, Wolfgeher D, Wu D & Kron SJ (2017) A signature of enhanced lipid metabolism, lipid peroxidation and aldehyde stress in therapy-induced senescence. *Cell Death Discovery* 3, 1–12.

Freund A, Laberge R-M, Demaria M & Campisi J (2012) Lamin B1 loss is a senescence-associated biomarker. *Mol. Biol. Cell* 23, 2066–2075.

Fuhrmann-Stroissnigg H, Ling YY, Zhao J, McGowan SJ, Zhu Y, Brooks RW, Grassi D, Gregg SQ, Stripay JL, Dorronsoro A, Corbo L, Tang P, Bukata C, Ring N, Giacca M, Li X, Tchkonia T, Kirkland JL, Niedernhofer LJ & Robbins PD (2017) Identification of HSP90 inhibitors as a novel class of senolytics. *Nature Communications* 8, 422.

Funayama R, Saito M, Tanobe H & Ishikawa F (2006) Loss of linker histone H1 in cellular senescence. *J Cell Biol* 175, 869–880.

Garbe JC, Bhattacharya S, Merchant B, Bassett E, Swisshelm K, Feiler HS, Wyrobek AJ & Stampfer MR (2009) Molecular Distinctions between Stasis and Telomere Attrition Senescence Barriers Shown by Long-term Culture of Normal Human Mammary Epithelial Cells. *Cancer Res* 69, 7557–7568.

Ghandi M, Huang FW, Jané-Valbuena J, Kryukov GV, Lo CC, McDonald ER, Barretina J, Gelfand ET, Bielski CM, Li H, Hu K, Andreev-Drakhlin AY, Kim J, Hess JM, Haas BJ, Aguet F, Weir BA, Rothberg MV, Paolella BR, Lawrence MS, Akbani R, Lu Y, Tiv HL, Gokhale PC, de Weck A, Mansour AA, Oh C, Shih J, Hadi K, Rosen Y, Bistline J, Venkatesan K, Reddy A, Sonkin D, Liu M, Lehar J, Korn JM, Porter DA, Jones MD, Golji J, Caponigro G, Taylor JE, Dunning CM, Creech AL, Warren AC, McFarland JM, Zamanighomi M, Kauffmann A, Stransky N, Imielinski M, Maruvka YE, Cherniack AD, Tsherniak A, Vazquez F, Jaffe JD, Lane AA, Weinstock DM, Johannessen CM, Morrissey MP, Stegmeier F, Schlegel R, Hahn WC, Getz G, Mills GB, Boehm JS, Golub TR, Garraway LA & Sellers WR (2019) Next-generation characterization of the Cancer Cell Line Encyclopedia. *Nature* 569, 503–508.

Golub TR, Slonim DK, Tamayo P, Huard C, Gaasenbeek M, Mesirov JP, Coller H, Loh ML, Downing JR, Caligiuri MA, Bloomfield CD & Lander ES (1999) Molecular classification of cancer: class discovery and class prediction by gene expression monitoring. *Science* 286, 531–537.

Gonskikh Y & Polacek N (2017) Alterations of the translation apparatus during aging and stress response. *Mechanisms of Ageing and Development* 168, 30–36.

Guerrero A, Herranz N, Sun B, Wagner V, Gallage S, Guiho R, Wolter K, Pombo J, Irvine EE, Innes AJ, Birch J, Glegola J, Manshaei S, Heide D, Dharmalingam G, Harbig J, Olona A, Behmoaras J, Dauch D, Uren AG, Zender L, Vernia S, Martínez-Barbera JP, Heikenwalder M, Withers DJ & Gil J (2019) Cardiac glycosides are broad-spectrum senolytics. *Nat Metab* 1, 1074–1088.

Heyn H, Li N, Ferreira HJ, Moran S, Pisano DG, Gomez A, Diez J, Sanchez-Mut JV, Setien F, Carmona FJ, Puca AA, Sayols S, Pujana MA, Serra-Musach J, Iglesias-Platas I, Formiga F, Fernandez AF, Fraga MF, Heath SC, Valencia A, Gut IG, Wang J & Esteller M (2012) Distinct

DNA methylomes of newborns and centenarians. *Proc. Natl. Acad. Sci. U.S.A.* 109, 10522–10527.

Hickson LJ, Langhi Prata LGP, Bobart SA, Evans TK, Giorgadze N, Hashmi SK, Herrmann SM, Jensen MD, Jia Q, Jordan KL, Kellogg TA, Khosla S, Koerber DM, Lagnado AB, Lawson DK, LeBrasseur NK, Lerman LO, McDonald KM, McKenzie TJ, Passos JF, Pignolo RJ, Pirtskhalava T, Saadiq IM, Schaefer KK, Textor SC, Victorelli SG, Volkman TL, Xue A, Wentworth MA, Wissler Gerdes EO, Zhu Y, Tchkonia T & Kirkland JL (2019) Senolytics decrease senescent cells in humans: Preliminary report from a clinical trial of Dasatinib plus Quercetin in individuals with diabetic kidney disease. *EBioMedicine* 47, 446–456.

Ivanov A, Pawlikowski J, Manoharan I, van Tuyn J, Nelson DM, Rai TS, Shah PP, Hewitt G, Korolchuk VI, Passos JF, Wu H, Berger SL & Adams PD (2013) Lysosome-mediated processing of chromatin in senescence. *J Cell Biol* 202, 129–143.

Jeon OH, David N, Campisi J & Elisseeff JH (2018) Senescent cells and osteoarthritis: a painful connection. *J. Clin. Invest.* 128, 1229–1237.

Jia J, Claude-Taupin A, Gu Y, Choi SW, Peters R, Bissa B, Mudd MH, Allers L, Pallikkuth S, Lidke KA, Salemi M, Phinney B, Mari M, Reggiori F & Deretic V (2020) Galectin-3 Coordinates a Cellular System for Lysosomal Repair and Removal. *Developmental Cell* 52, 69-87.e8.

Jun J-I & Lau LF (2010) The matricellular protein CCN1 induces fibroblast senescence and restricts fibrosis in cutaneous wound healing. *Nat. Cell Biol.* 12, 676–685.

Kane AE & Sinclair DA (2019) Epigenetic changes during aging and their reprogramming potential. *Critical Reviews in Biochemistry and Molecular Biology* 54, 61–83.

Kim W, Kim R, Park G, Park J-W & Kim J-E (2012) Deficiency of H3K79 Histone Methyltransferase Dot1-like Protein (DOT1L) Inhibits Cell Proliferation. *J Biol Chem* 287, 5588–5599.

Kirkland JL & Tchkonia T (2020) Senolytic Drugs: From Discovery to Translation. *J. Intern. Med.*

Kirkland JL, Tchkonia T, Zhu Y, Niedernhofer LJ & Robbins PD (2017) The Clinical Potential of Senolytic Drugs. *J Am Geriatr Soc* 65, 2297–2301.

Klement K, Melle C, Murzik U, Diekmann S, Norgauer J & Hemmerich P (2012) Accumulation of annexin A5 at the nuclear envelope is a biomarker of cellular aging. *Mechanisms of Ageing and Development* 133, 508–522.

Kochetkova EY, Blinova GI, Bystrova OA, Martynova MG, Pospelov VA & Pospelova TV (2017) Targeted elimination of senescent Ras-transformed cells by suppression of MEK/ERK pathway. *Aging (Albany NY)* 9, 2352–2375.

Krishnamurthy J, Torrice C, Ramsey MR, Kovalev GI, Al-Regaiey K, Su L & Sharpless NE (2004) Ink4a/Arf expression is a biomarker of aging. *J. Clin. Invest.* 114, 1299–1307.

Kwan S-Y, Sheel A, Song C-Q, Zhang X-O, Jiang T, Dang H, Cao Y, Ozata DM, Mou H, Yin H, Weng Z, Wang XW & Xue W (2020) Depletion of TRRAP Induces p53-Independent Senescence in Liver Cancer by Down-Regulating Mitotic Genes. *Hepatology* 71, 275–290.

Lee BY, Han JA, Im JS, Morrone A, Johung K, Goodwin EC, Kleijer WJ, DiMaio D & Hwang ES (2006) Senescence-associated beta-galactosidase is lysosomal beta-galactosidase. *Aging Cell* 5, 187–195.

Lehallier B, Gate D, Schaum N, Nanasi T, Lee SE, Yousef H, Moran Losada P, Berdnik D, Keller A, Verghese J, Sathyan S, Franceschi C, Milman S, Barzilai N & Wyss-Coray T (2019) Undulating changes in human plasma proteome profiles across the lifespan. *Nat. Med.* 25, 1843–1850.

Lessard F, Igelmann S, Trahan C, Huot G, Saint-Germain E, Mignacca L, Toro ND, Lopes-Paciencia S, Calvé BL, Montero M, Deschênes-Simard X, Bury M, Moiseeva O, Rowell M-C, Zorca CE, Zenklusen D, Brakier-Gingras L, Bourdeau V, Oeffinger M & Ferbeyre G (2018) Senescence-associated ribosome biogenesis defects contributes to cell cycle arrest through the Rb pathway. *Nature Cell Biology* 20, 789–799.

Moghieb A, Bramlett HM, Das JH, Yang Z, Selig T, Yost RA, Wang MS, Dietrich WD & Wang KKW (2016) Differential Neuroproteomic and Systems Biology Analysis of Spinal Cord Injury. *Mol. Cell Proteomics* 15, 2379–2395.

Mullani N, Porozhan Y, Costallat M, Batsché E, Goodhardt M, Cenci G, Mann C & Muchardt C (2020) Reduced RNA turnover as a driver of cellular senescence. *bioRxiv,* 800128.

Muñoz-Espín D, Cañamero M, Maraver A, Gómez-López G, Contreras J, Murillo-Cuesta S, Rodríguez-Baeza A, Varela-Nieto I, Ruberte J, Collado M & Serrano M (2013) Programmed cell senescence during mammalian embryonic development. *Cell* 155, 1104–1118.

Muñoz-Espín D, Rovira M, Galiana I, Giménez C, Lozano-Torres B, Paez-Ribes M, Llanos S, Chaib S, Muñoz-Martín M, Ucero AC, Garaulet G, Mulero F, Dann SG, VanArsdale T, Shields DJ, Bernardos A, Murguía JR, Martínez-Máñez R & Serrano M (2018) A versatile drug delivery system targeting senescent cells. *EMBO Mol Med* 10.

Niu H, Qian L, Sun B, Liu W, Wang F, Wang Q, Ji X, Luo Y, Nesa EU, Lou H & Yuan H (2019) Inactivation of TFEB and NF-κB by marchantin M alleviates the chemotherapy-driven pro-tumorigenic senescent secretion. *Acta Pharm Sin B* 9, 923–936.

Nixon RA, Cataldo AM & Mathews PM (2000) The Endosomal-Lysosomal System of Neurons in Alzheimer's Disease Pathogenesis: A Review. *Neurochem Res* 25, 1161–1172.

Nusinow DP, Szpyt J, Ghandi M, Rose CM, McDonald ER, Kalocsay M, Jané-Valbuena J, Gelfand E, Schweppe DK, Jedrychowski M, Golji J, Porter DA, Rejtar T, Wang YK, Kryukov GV, Stegmeier F, Erickson BK, Garraway LA, Sellers WR & Gygi SP (2020) Quantitative Proteomics of the Cancer Cell Line Encyclopedia. *Cell* 180, 387-402.e16.

Park JT, Lee Y-S, Cho KA & Park SC (2018) Adjustment of the lysosomal-mitochondrial axis for control of cellular senescence. *Ageing Research Reviews* 47, 176–182.

Pavlicek D, Krebs J, Capossela S, Bertolo A, Engelhardt B, Pannek J & Stoyanov J (2017) Immunosenescence in persons with spinal cord injury in relation to urinary tract infections -a cross-sectional study-. *Immunity & Ageing* 14, 22.

Perez-Riverol Y, Csordas A, Bai J, Bernal-Llinares M, Hewapathirana S, Kundu DJ, Inuganti A, Griss J, Mayer G, Eisenacher M, Pérez E, Uszkoreit J, Pfeuffer J, Sachsenberg T, Yılmaz Ş, Tiwary S,

Cox J, Audain E, Walzer M, Jarnuczak AF, Ternent T, Brazma A & Vizcaíno JA (2019) The PRIDE database and related tools and resources in 2019: improving support for quantification data. *Nucleic Acids Res* 47, D442–D450.

Sadaie M, Salama R, Carroll T, Tomimatsu K, Chandra T, Young ARJ, Narita M, Pérez-Mancera PA, Bennett DC, Chong H, Kimura H & Narita M (2013) Redistribution of the Lamin B1 genomic binding profile affects rearrangement of heterochromatic domains and SAHF formation during senescence. *Genes Dev* 27, 1800–1808.

Shah PP, Donahue G, Otte GL, Capell BC, Nelson DM, Cao K, Aggarwala V, Cruickshanks HA, Rai TS, McBryan T, Gregory BD, Adams PD & Berger SL (2013) Lamin B1 depletion in senescent cells triggers large-scale changes in gene expression and the chromatin landscape. *Genes Dev* 27, 1787–1799.

Shang D, Sun D, Shi C, Xu J, Shen M, Hu X, Liu H & Tu Z (2020) Activation of epidermal growth factor receptor signaling mediates cellular senescence induced by certain pro-inflammatory cytokines. *Aging Cell* 19, e13145.

Stampfer MR, LaBarge MA & Garbe JC (2013) An Integrated Human Mammary Epithelial Cell Culture System for Studying Carcinogenesis and Aging. In *Cell and Molecular Biology of Breast Cancer*. Humana Press, Totowa, NJ, pp.323–361. Available at: https://link.springer.com/chapter/10.1007/978-1-62703-634-4_15 [Accessed March 14, 2018].

Stoka V, Turk V & Turk B (2016) Lysosomal cathepsins and their regulation in aging and neurodegeneration. *Ageing Research Reviews* 32, 22–37.

Storer M, Mas A, Robert-Moreno A, Pecoraro M, Ortells MC, Di Giacomo V, Yosef R, Pilpel N, Krizhanovsky V, Sharpe J & Keyes WM (2013) Senescence is a developmental mechanism that contributes to embryonic growth and patterning. *Cell* 155, 1119–1130.

Subramanian A, Tamayo P, Mootha VK, Mukherjee S, Ebert BL, Gillette MA, Paulovich A, Pomeroy SL, Golub TR, Lander ES & Mesirov JP (2005) Gene set enrichment analysis: A knowledge-based approach for interpreting genome-wide expression profiles. *PNAS* 102, 15545–15550.

Swenson BL, Meyer CF, Bussian TJ & Baker DJ (2019) Senescence in aging and disorders of the central nervous system. *Translational Medicine of Aging* 3, 17–25.

Tajima K, Matsuda S, Yae T, Drapkin BJ, Morris R, Boukhali M, Niederhoffer K, Comaills V, Dubash T, Nieman L, Guo H, Magnus NKC, Dyson N, Shioda T, Haas W, Haber DA & Maheswaran S (2019) SETD1A protects from senescence through regulation of the mitotic gene expression program. *Nature Communications* 10, 2854.

Takano M, Kawabata S, Shibata S, Yasuda A, Nori S, Tsuji O, Nagoshi N, Iwanami A, Ebise H, Horiuchi K, Okano H & Nakamura M (2017) Enhanced Functional Recovery from Spinal Cord Injury in Aged Mice after Stem Cell Transplantation through HGF Induction. *Stem Cell Reports* 8, 509–518.

Tanaka T, Biancotto A, Moaddel R, Moore AZ, Gonzalez-Freire M, Aon MA, Candia J, Zhang P, Cheung F, Fantoni G, Semba RD & Ferrucci L (2018) Plasma proteomic signature of age in healthy humans. *Aging Cell* 17. Available at: https://www.ncbi.nlm.nih.gov/pmc/articles/PMC6156492/ [Accessed September 20, 2020].

Tchkonia T, Zhu Y, van Deursen J, Campisi J & Kirkland JL (2013) Cellular senescence and the senescent secretory phenotype: therapeutic opportunities. *J. Clin. Invest.* 123, 966–972.

Thompson PJ, Shah A, Ntranos V, Gool FV, Atkinson M & Bhushan A (2019) Targeted Elimination of Senescent Beta Cells Prevents Type 1 Diabetes. *Cell Metabolism* 29, 1045-1060.e10.

Tominaga K (2015) The emerging role of senescent cells in tissue homeostasis and pathophysiology. *Pathobiol Aging Age Relat Dis* 5, 27743.

Valentijn FA, Falke LL, Nguyen TQ & Goldschmeding R (2018) Cellular senescence in the aging and diseased kidney. *J Cell Commun Signal* 12, 69–82.

Wang AS, Ong PF, Chojnowski A, Clavel C & Dreesen O (2017) Loss of lamin B1 is a biomarker to quantify cellular senescence in photoaged skin. *Sci Rep* 7. Available at: https://www.ncbi.nlm.nih.gov/pmc/articles/PMC5688158/ [Accessed September 20, 2020].

Webb-Robertson B-JM, Wiberg HK, Matzke MM, Brown JN, Wang J, McDermott JE, Smith RD, Rodland KD, Metz TO, Pounds JG & Waters KM (2015) Review, Evaluation, and Discussion of the Challenges of Missing Value Imputation for Mass Spectrometry-Based Label-Free Global Proteomics. *J. Proteome Res.* 14, 1993–2001.

Xu M, Pirtskhalava T, Farr JN, Weigand BM, Palmer AK, Weivoda MM, Inman CL, Ogrodnik MB, Hachfeld CM, Fraser DG, Onken JL, Johnson KO, Verzosa GC, Langhi LGP, Weigl M, Giorgadze N, LeBrasseur NK, Miller JD, Jurk D, Singh RJ, Allison DB, Ejima K, Hubbard GB, Ikeno Y, Cubro H, Garovic VD, Hou X, Weroha SJ, Robbins PD, Niedernhofer LJ, Khosla S, Tchkonia T & Kirkland JL (2018) Senolytics improve physical function and increase lifespan in old age. *Nature Medicine* 24, 1246–1256.

Yevshin I, Sharipov R, Kolmykov S, Kondrakhin Y & Kolpakov F (2019) GTRD: a database on gene transcription regulation—2019 update. *Nucleic Acids Res* 47, D100–D105.

Yousefzadeh MJ, Zhu Y, McGowan SJ, Angelini L, Fuhrmann-Stroissnigg H, Xu M, Ling YY, Melos KI, Pirtskhalava T, Inman CL, McGuckian C, Wade EA, Kato JI, Grassi D, Wentworth M, Burd CE, Arriaga EA, Ladiges WL, Tchkonia T, Kirkland JL, Robbins PD & Niedernhofer LJ (2018) Fisetin is a senotherapeutic that extends health and lifespan. *EBioMedicine* 36, 18–28.

Zhang B, Wang J, Wang X, Zhu J, Liu Q, Shi Z, Chambers MC, Zimmerman LJ, Shaddox KF, Kim S, Davies SR, Wang S, Wang P, Kinsinger CR, Rivers RC, Rodriguez H, Townsend RR, Ellis MJC, Carr SA, Tabb DL, Coffey RJ, Slebos RJC, Liebler DC & the NCI Cptac (2014) Proteogenomic characterization of human colon and rectal cancer. *Nature* 513, 382–387.

Zhu Y, Orre LM, Tran YZ, Mermelekas G, Johansson HJ, Malyutina A, Anders S & Lehtiö J (2020) DEqMS: A Method for Accurate Variance Estimation in Differential Protein Expression Analysis. *Molecular & Cellular Proteomics* 19, 1047–1057.

Zhu Y, Tchkonia T, Fuhrmann-Stroissnigg H, Dai HM, Ling YY, Stout MB, Pirtskhalava T, Giorgadze N, Johnson KO, Giles CB, Wren JD, Niedernhofer LJ, Robbins PD & Kirkland JL (2016) Identification of a novel senolytic agent, navitoclax, targeting the Bcl-2 family of anti-apoptotic factors. *Aging Cell* 15, 428–435.

Zhu Y, Tchkonia T, Pirtskhalava T, Gower AC, Ding H, Giorgadze N, Palmer AK, Ikeno Y, Hubbard GB, Lenburg M, O'Hara SP, LaRusso NF, Miller JD, Roos CM, Verzosa GC, LeBrasseur NK, Wren JD, Farr JN, Khosla S, Stout MB, McGowan SJ, Fuhrmann-Stroissnigg H, Gurkar AU, Zhao J, Colangelo D, Dorronsoro A, Ling YY, Barghouthy AS, Navarro DC, Sano T, Robbins PD, Niedernhofer LJ & Kirkland JL (2015) The Achilles' heel of senescent cells: from transcriptome to senolytic drugs. *Aging Cell* 14, 644–658.
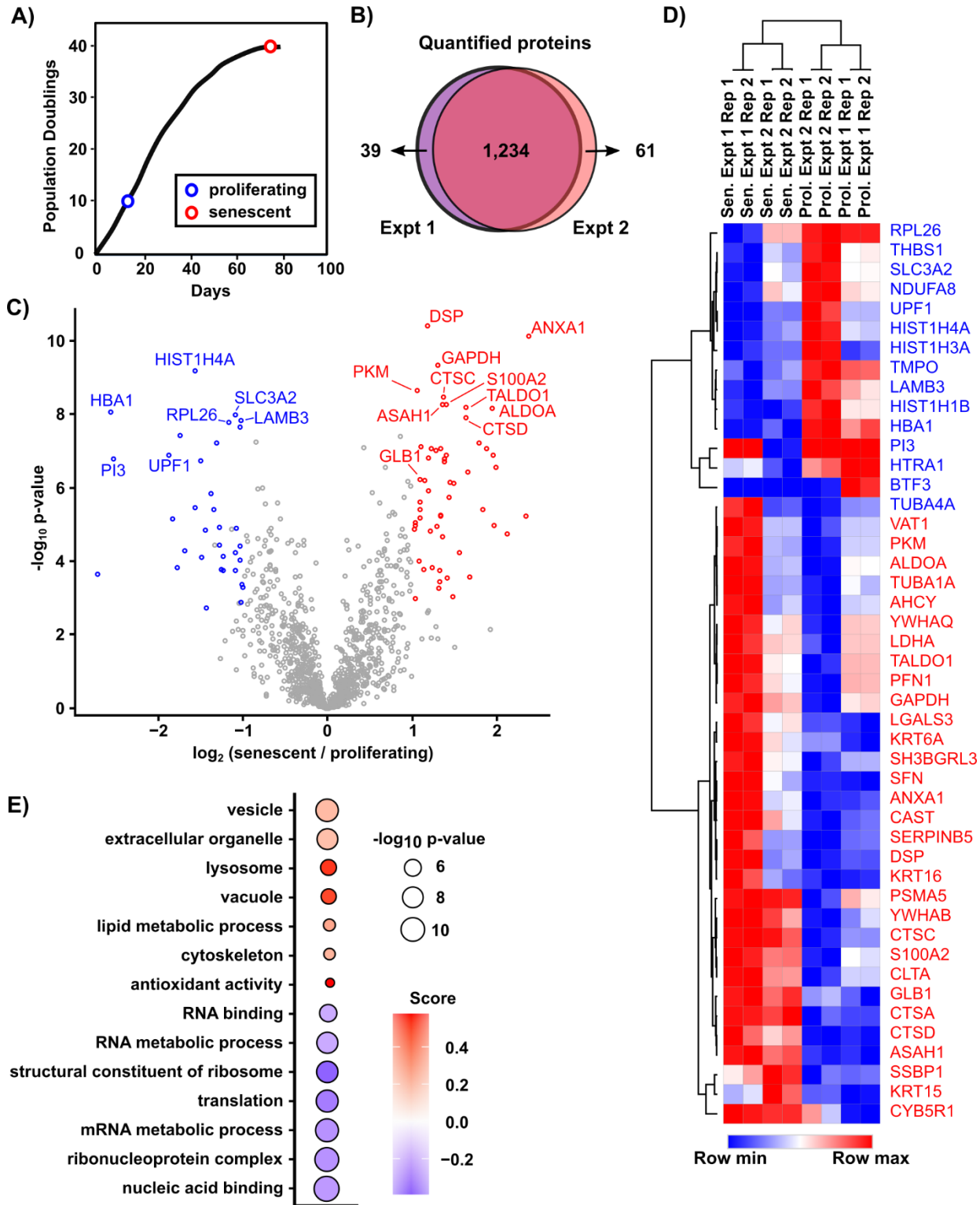
Figures

Figure 1: Replicative senescence alters the HMEC proteome

A. Primary HMECs proliferate for ~40 population doublings (PD). Proteomics samples were collected at PD ~10 and PD ~40 to compare proliferating and senescent HMECs. At each time, two biologically independent replicates were collected. The growth curve represents the approximate collection times of the proliferating and senescent samples.

B. Number of proteins quantified in two independent biological replicates as described in A. Proteomics sample prep was performed as two independent experiments with one proliferating and one senescent sample in each experiment. For each experiment, duplicate injections (technical replicates) were run from each proliferating and senescent sample.

C. Volcano plot representing average of $\log_2$ fold change of protein levels comparing senescent versus proliferating HMECs plotted against the -$\log_{10}$ p-value. Red and blue denote the 55 significantly upregulated and 34 significantly down-regulated proteins, respectively (FDR-corrected p-value < 0.01 and average absolute $\log_2$ fold change > 1).

D. Hierarchical clustering of protein expression levels for differentially expressed proteins in senescent (Sen.) and proliferating (Prol.) HMECs across biological (Expt) and technical replicates (Rep). Proteins with FDR-corrected p-value < 0.0001 and average absolute $\log_2$ fold change > 1 are shown.

E. Gene Ontology enrichment analysis performed in Perseus software (1D-enrichment analysis). The color of the circle denotes the enrichment score, and the size of the circle denotes the statistical significance of the enrichment, as shown in the legend.
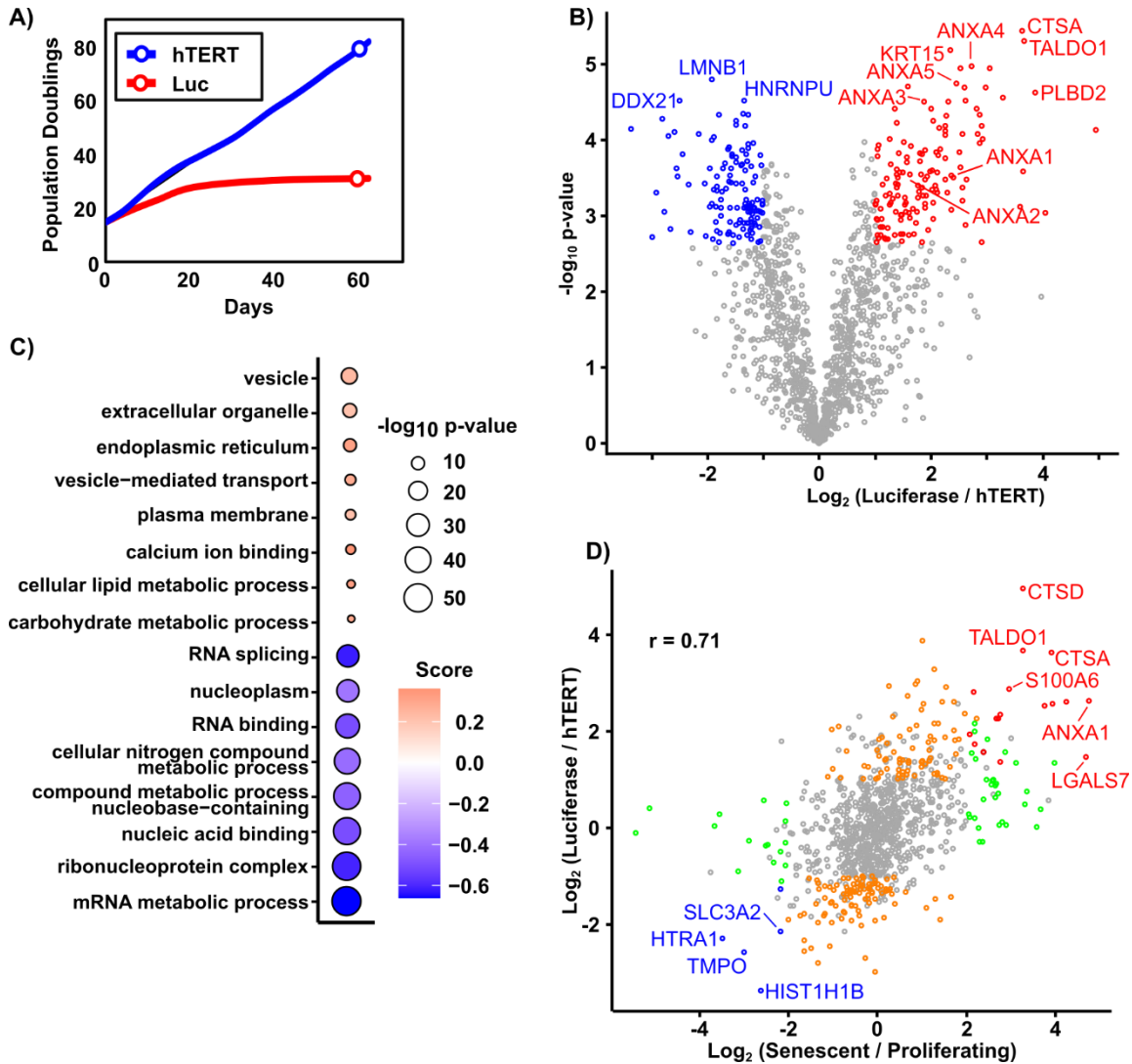
Figure 2: The proteome of hTERT-immortalized HMECs resembles that of proliferating HMECs

A. Representative growth curve for HMECs infected with either luciferase (negative control, senescent) or hTERT (immortalized). Circles represent the approximate time of sample collection. One biological replicate was collected and analyzed in technical duplicate by LC-MS proteomics.

B. Volcano plot representing log_2 fold change of protein levels for luciferase versus hTERT plotted against the $-log_{10}$ p-value. Red and blue denote significantly up- and down-regulated proteins, respectively (FDR-corrected p-value < 0.01 and absolute log_2 fold change > 1).

C. Gene Ontology enrichment analysis performed in Perseus software (1D-enrichment analysis). The color of the circle denotes the enrichment score, and the size of the circle denotes the statistical significance of the enrichment, as shown in the legend.

D. Comparison of protein expression changes in luciferase versus hTERT HMECs against senescent versus proliferating HMECs (i.e., replicative senescence). Red and blue circles denote proteins that were significantly upregulated and downregulated, respectively, in both data sets (FDR corrected p-value < 0.01, and absolute $\log_2$ fold change > 1). Green and orange circles represent proteins that were significantly changed in senescent versus proliferating cells but not in luciferase versus hTERT cells or in luciferase versus hTERT cells but not senescent versus proliferating cells, respectively. The Pearson correlation coefficient is shown.
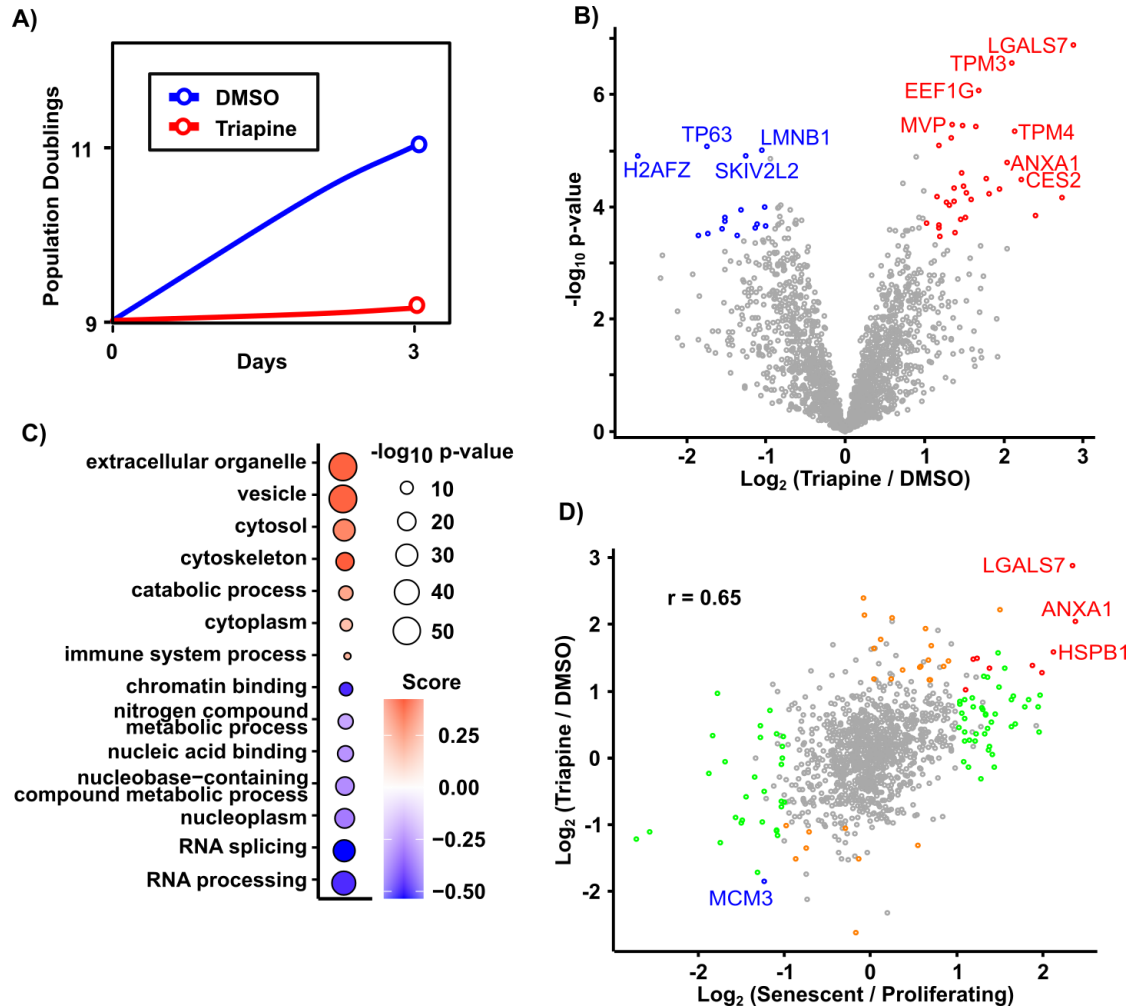
Figure 3: The proteome of RRM2 inhibition-induced senescence resembles that of replicative senescence

A. Representative growth curve for HMECs treated with either DMSO (negative control, proliferating) or triapine (senescent). Circles represent the approximate time of sample collection. Three biological replicates were collected and analyzed in technical singlicate by LC-MS proteomics.

B. Volcano plot representing $\log_2$ fold change of protein levels for triapine versus DMSO plotted against the $-\log_{10}$ p-value. Red and blue denote significantly up- and down-regulated proteins, respectively (FDR-corrected p-value < 0.01 and absolute $\log_2$ fold change > 1).

C. Gene Ontology enrichment analysis performed in Perseus software (1D-enrichment analysis). The color of the circle denotes the enrichment score, and the size of the circle denotes the statistical significance of the enrichment, as shown in the legend.

D. Comparison of protein expression changes in triapine versus DMSO HMECs against senescent versus proliferating HMECs (i.e., replicative senescence). Red and blue circles denote proteins that were significantly upregulated and downregulated, respectively, in both data sets (FDR corrected p-value < 0.01, and absolute $\log_2$ fold change > 1). Green and orange circles represent proteins that were significantly changed in senescent versus proliferating cells but not in triapine versus DMSO cells or in triapine versus DMSO cells but not senescent versus proliferating cells, respectively. The Pearson correlation coefficient is shown.
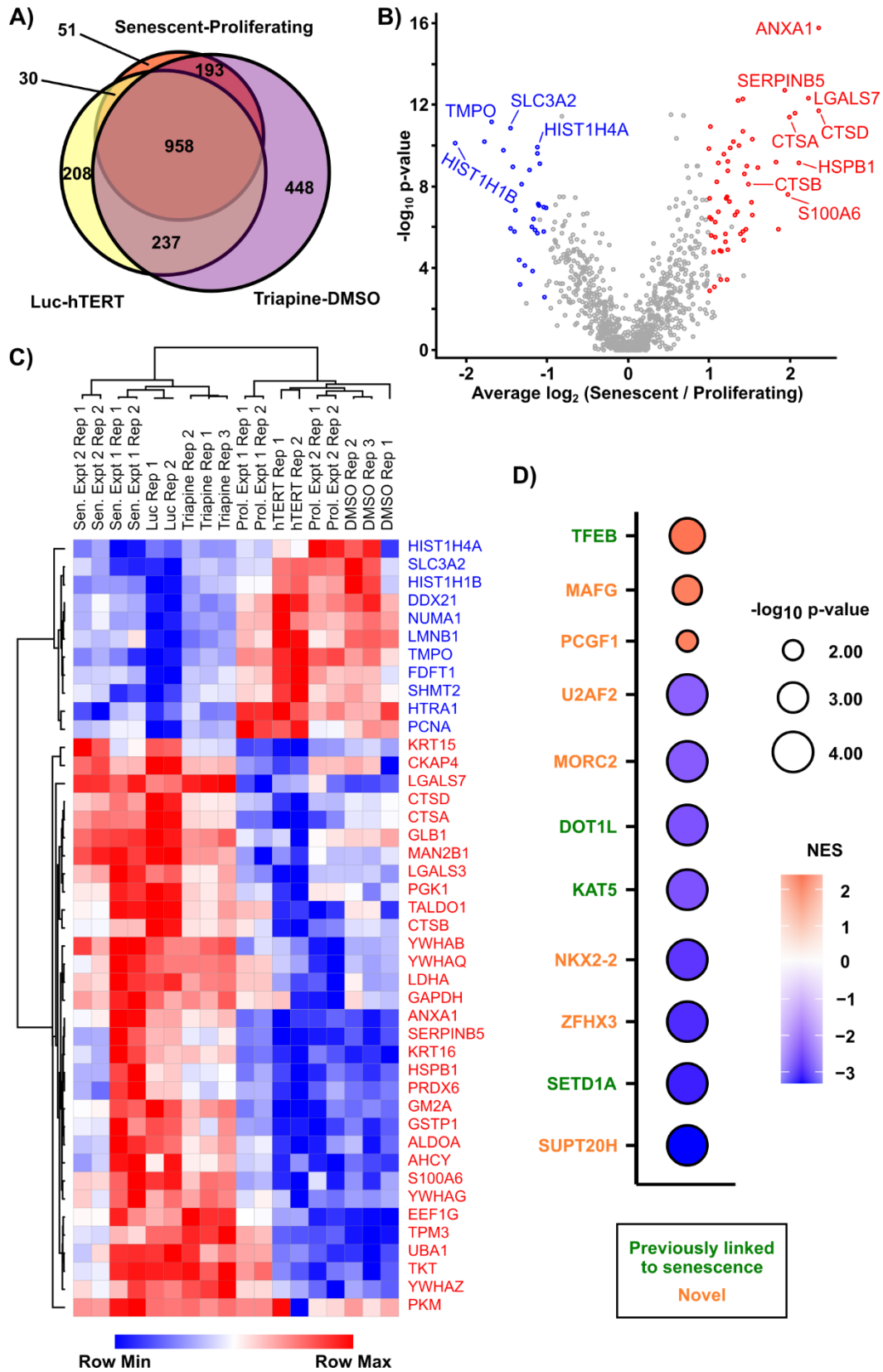
Figure 4: Data integration identifies a proteomic signature of HMEC senescence

A. Venn diagram showing the overlap in the number of proteins identified in each dataset: senescent versus proliferating HMECs (Fig. 1), luciferase- versus hTERT-expressing HMECs (Fig. 2), and triapine- versus DMSO-treated HMECs (Fig. 3).

B. Volcano plot representing average of $\log_2$ (senescent / proliferating) vs. -$\log_{10}$ p-value combined statistical significance of data from 3 datasets shown on Figures 1-3. Red and blue circles show proteins that were consistently up- or down-regulated upon integration of the 3 datasets, respectively (FDR corrected p-value < 0.01, average absolute $\log_2$ fold change > 1).

C. Hierarchical clustering of significantly altered proteins across all 3 datasets. Proteins with FDR corrected p-value < 1 x 10^{-6} and average absolute log2 fold change > 1 are shown. All biological and technical replicates are shown.

D. Gene Set Enrichment Analysis (GSEA) to identify enrichment of transcription factor targets gene lists. The color of the circle denotes the enrichment score, and the size of the circle denotes the statistical significance of the enrichment, as shown in the legend.
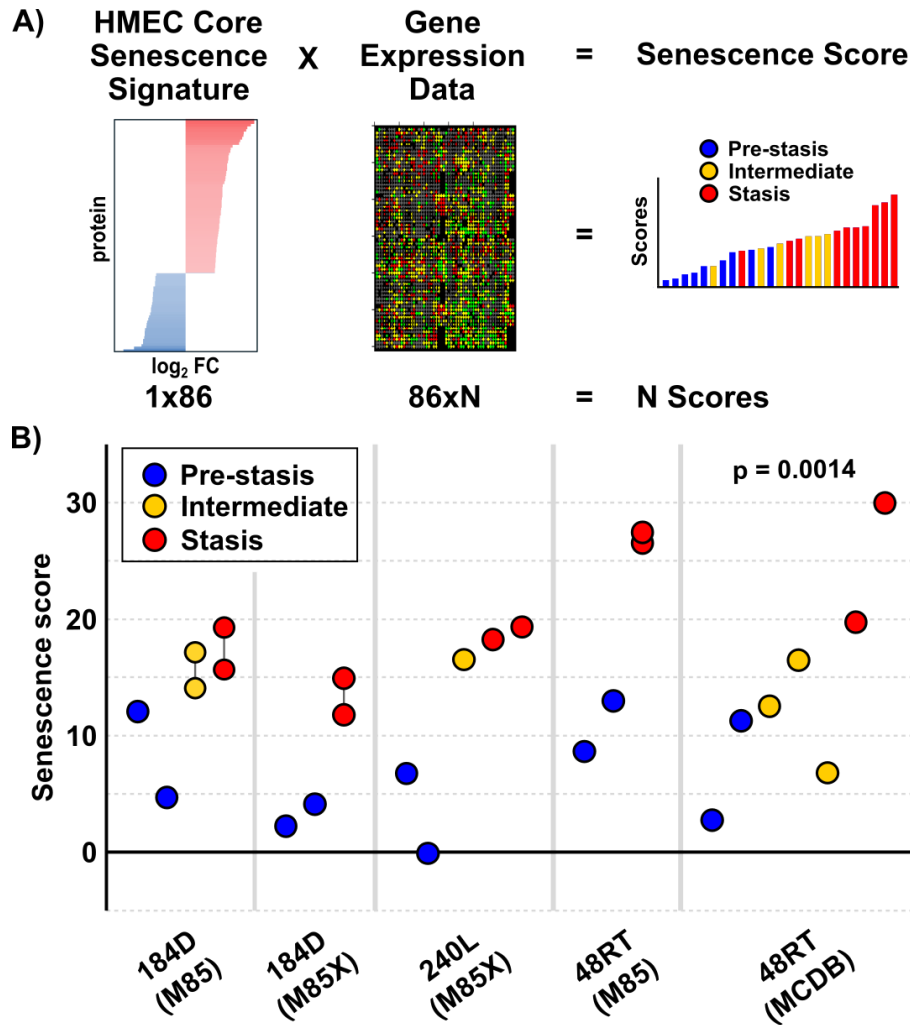
Figure 5: Defining a senescence score that predicts HMECs senescence

A. Schematic representing calculation of HMEC senescence score using weighted voting (Golub et al. 1999) The proteomic signature of HMEC senescence (Fig. 4C) was used as voting weights (log_2 fold change of protein expression comparing senescent and proliferating HMEC, 86 proteins total). Weights were multiplied by gene expression data to calculate a HMEC senescence score for each sample.

B. Gene expression data from five independent HMEC cell lines (Garbe et al. 2009) was analyzed using weighted voting as in panel A. Samples for each cell line are arranged in increasing passage number and colored according to pre-stasis (i.e., proliferating), intermediate, or stasis (i.e., senescent) as in the original publication. M85, M85X, and MCDB

represent different media formulations. Samples profiled at the same passage are connected

by a thin dark gray line. p = 0.0014 comparing the senescence scores from pre-stasis and
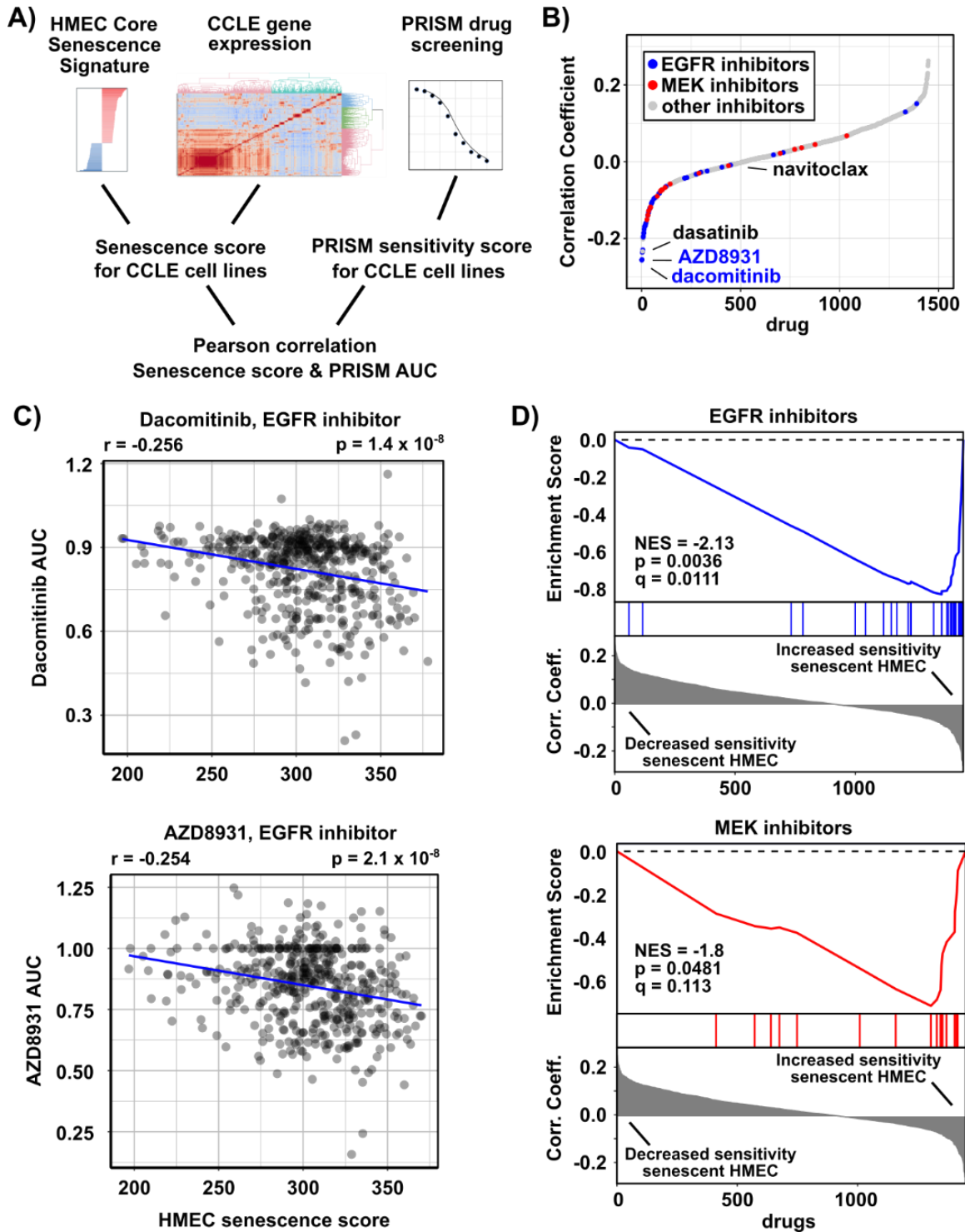
stasis using a paired (by cell line) t-test.

Figure 6: Large-scale drug screening databases predict that EGFR inhibitors, MEK inhibitors, and dasatinib are senolytic compounds in HMECs

A. Schematic of analysis workflow. The senescence score was calculated for ~500 cancer cell lines present in both the CCLE and the DepMap drug screening databases using the proteomic signature of HMEC senescence. For each drug, we calculated a Pearson correlation coefficient between PRISM AUC and senescence scores. Because smaller AUC indicates increased sensitivity to drug treatment, negative correlation coefficients indicate increased toxicity to senescent cells.

B. Waterfall plot of the Pearson correlation coefficients for all 1,448 drug sensitivities correlated with the HMEC senescence score. Red and blue indicate EGFR and MEK inhibitors, respectively. The tyrosine kinase dasatinib and the BCL-2 / BCL-xL inhibitor navitoclax are also indicated.

C. The EGFR inhibitors dacomitinib and AZD8931 were predicted to be the most senolytic drugs for HMECs. P-values shown have been FDR corrected using the Benjamini-Hochberg method. r, Pearson correlation coefficient.

D. Drug Set Enrichment Analysis (DrugSEA) revealed that EGFR and MEK inhibitors are enriched among predicted senolytic drugs for HMECs. p, permutation p-value. q, false discovery rate.